Original Article

Wnt10b Inhibits Obesity in *ob/ob* and Agouti Mice

Wendy S. Wright,[1] Kenneth A. Longo,[1] Vernon W. Dolinsky,[1] Isabelle Gerin,[1] Sona Kang,[1] Christina N. Bennett,[1] Shian-Huey Chiang,[1] Tyler C. Prestwich,[1] Catherine Gress,[2] Charles F. Burant,[1,3] Vedrana S. Susulic,[2] and Ormond A. MacDougald[1,3]

The Wnt family of secreted signaling molecules has profound effects on diverse developmental processes, including the fate of mesenchymal progenitors. While activation of Wnt signaling blocks adipogenesis, inhibition of endogenous Wnt/β-catenin signaling by Wnt10b promotes spontaneous preadipocyte differentiation. Transgenic mice with expression of Wnt10b from the FABP4 promoter (FABP4-Wnt10b) have less adipose tissue when maintained on a normal chow diet and are resistant to diet-induced obesity. Here we demonstrate that FABP4-Wnt10b mice largely avert weight gain and metabolic abnormalities associated with genetic obesity. FABP4-Wnt10b mice do not gain significant body weight on the *ob/ob* background, and at 8 weeks of age, they have an ~70% reduction in visceral and subcutaneous adipose tissues compared with *ob/ob* mice. Similarly, on the lethal yellow agouti (A^y) background, FABP4-Wnt10b mice have 50–70% less adipose tissue weight and circulating leptin at 5 months of age. Wnt10b-*Ay* mice are more glucose tolerant and insulin sensitive than A^y controls, perhaps due to reduced expression and circulation of resistin. Reduced expression of inflammatory cytokines may also contribute to improved glucose homeostasis. *Diabetes* 56:295–303, 2007

Preadipocyte fate is controlled by both external and endogenously produced factors, and the balance between stimulatory and repressive forces influences whether cells remain quiescent, replicate, or differentiate into adipocytes (1). Wnt signaling is one of the endogenous inhibitory forces that regulate differentiation and other aspects of adipocyte biology (2–6). Wnts comprise a family of secreted lipid-modified glycoproteins that act through autocrine and paracrine mechanisms to influence many developmental and cellular processes. Although Wnts can inhibit preadipocyte differentiation through pathways that are dependent or independent of β-catenin (7), genetic evidence suggests that β-catenin signaling is the predominant regulator of adipogenesis. In the Wnt/β-catenin (i.e., canonical) pathway, Wnts bind to frizzled receptors and LDL receptor–related protein coreceptors to initiate intracellular signaling through disheveled and axin (8,9). This signal disrupts the complex of proteins containing glycogen synthase kinase 3 and β-catenin, resulting in inhibition of glycogen synthase kinase 3 and hypophosphorylation of its substrate, β-catenin. After stabilization in cytosol and translocation to the nucleus, β-catenin binds to T-cell factor/lymphoid-enhancing factors and other transcription factors to mediate effects of Wnt on gene expression.

In addition to regulating preadipocyte differentiation, Wnt/β-catenin signaling is an important regulator of mesenchymal cell fate (10). In several pluripotent in vitro models, activation of Wnt signaling stimulates osteoblastogenesis and inhibits adipogenesis (11–13). In mice, activation of Wnt signaling in adipocytes with Wnt10b expressed from the FABP4 promoter results in 50% less white adipose tissue and a complete lack of brown adipose development (14). In addition, FABP4-Wnt10b mice are resistant to diet-induced obesity and exhibit improved glucose tolerance and insulin sensitivity. The FABP4 promoter is also expressed in marrow, where Wnt10b increases the amount of trabecular bone and protects mice against loss of bone associated with estrogen depletion or aging. Similar results are observed with pharmacological activation of Wnt signaling. Treatment of mice with lithium, which activates the Wnt/β-catenin pathway by inhibiting glycogen synthase kinase 3, stimulates bone formation and inhibits development of marrow adipocytes (15). While disruption of a Wnt inhibitor such as secreted frizzled-related protein-1 increases bone formation and inhibits accumulation of total body lipid in older male mice (16), elevated expression of secreted frizzled-related protein-5 in adipose tissue may stimulate accumulation of fat mass (17).

While activation of Wnt/β-catenin signaling blocks adipogenesis, inhibition of endogenous Wnt signaling promotes adipogenesis, providing strong evidence that Wnts act as a brake to preadipocyte differentiation (2,4,18). Wnt10b appears to contribute to this endogenous inhibitory activity because it strongly blocks adipogenesisis and because Wnt10b is expressed in preadipocytes and stromal vascular cells but not in differentiated adipocytes. Furthermore, loss of Wnt10b in myoblasts with aging or in $Wnt10b^{-/-}$ mice is associated with increased adipogenic potential in myoblasts and acquisition of adipocyte characteristics during myofiber regeneration (19,20). Conversely, induction of Wnt10b expression by mechanical stretch inhibits adipogenesis of myoblasts (21). Although an obese individual lacking Wnt10b has been character-

From the [1]Department of Molecular and Integrative Physiology, University of Michigan, Ann Arbor, Michigan; [2]Centocor, Horsham, Pennsylvania; and the [3]Department of Internal Medicine, University of Michigan, Ann Arbor, Michigan.

Address correspondence and reprint requests to Ormond A. MacDougald, Department of Molecular and Integrative Physiology, 7620 Medical Science II, 1301 E. Catherine Dr., Ann Arbor, MI 48109-0622. E-mail: macdouga@umich.edu.

Received for publication 25 September 2006 and accepted in revised form 1 November 2006.

W.S.W. and K.A.L. contributed equally to this work.

DEXA, dual-energy X-ray absorptiometry; iNOS, inducible nitric oxide synthase; MCP, monocyte chemotactic protein; TNF, tumor necrosis factor.

DOI: 10.2337/db06-1339

TABLE 1
Primer sequences used for quantitative RT-PCR

Gene	Forward primer 5′–3′	Reverse primer 5′-3′
18S rRNA	cgc ttc ctt acc tgg ttg at	gag cga cca aag gaa cca ta
Adiponectin	aag aag gac aag gcc gtt ctc tt	gct atg ggt agt tgc agt cag tt
C/EBPα	tgg aca aga aca gca acg ag	tca ctg gtc atc tcc agc ac
F4/80	ctt tgg cta tgg gct tcc agt c	gca agg agg aca gag ttt atc
FABP4	tgg aag ctt gtc tcc agt ga	aat ccc cat tta cgc tga tg
FAS	gaa ccc tga ggg tcc tac cc	caa gga aca gag gcc gct c
FSP27	gcc agg ccc tgt cgt gt	gct gtg agc cat gat gcc tt
iNOS	aat ctt gga gcg agt tgt gg	cag gaa gta ggt gag ggc tg
Leptin	gac acc aaa acc ctc at	cag tgt ctg gtc cat ct
LPL	tgg aga agc cat ccg tgt g	tca tgc gag cac ttc acc ag
MCP-1	ctt ctg ggc ctg ctg ttc a	cca gcc tac tca ttg gga tca
PPARγ	gga aag aca acg gac aaa tca c	tac gga tcg aaa ctg gca c
Resistin	aag aag gag ctg tgg gac agg	cag cag ttc agg gac aag gaa
TNF-α	gga caa ggc tgc ccc gac ta	ctt ggg gca ggg gct ctt gac

C/EBP, CCAAT/enhancer-binding protein; FABP, fatty acid–binding protein 4; FAS, fatty acid synthase; FSP, fat-specific protein; LPL, lipoprotein lipase; PPAR, peroxisome proliferator–activated receptor.

ized (22), linkage of Wnt10b to increased susceptibility was not possible. Our preliminary analysis of Wnt10b$^{-/-}$ mice has not revealed an adipose tissue phenotype, perhaps suggesting that additional Wnts regulate adipogenesis. This notion is supported by recent work from Kahn and colleagues (23,24) indicating that Wnt10a and Wnt6 determine whether precursor cells undergo brown adipogenesis. In addition, based on analyses of human mutations associated with type 2 diabetes, Kawazawa and colleagues (25,26) reported that Wnt5b is transiently induced during adipogenesis and increases preadipocyte differentiation by stimulating turnover of β-catenin. Thus, Wnt activity in mesenchymal precursors is complex, with contributions from multiple Wnts with differential effects on β-catenin signaling. Additional layers of regulation and complexity arise from highly regulated expression of secreted and intracellular regulators of Wnt signaling. Although much has yet to be discovered about how Wnts regulate adipose development, the conversion of myometrial smooth muscle to adipose in mice with loss of β-catenin in this tissue indicates that the Wnt/β-catenin pathway is a critical regulator of adipogenesis and mesenchymal cell fate in vivo (27).

Expression of Wnt10b blocks adipose tissue development and protects transgenic mice against diet-induced obesity (14). In this study, we explore whether Wnt10b protects against genetic obesity due to mutations causing leptin deficiency (*ob/ob*) or ectopic expression of agouti (A^y). The *ob/ob* model arose from a spontaneous deleterious mutation in the leptin gene. Mice homozygous for the *ob/ob* mutation are characterized by hyperphagia and hypometabolism, leading to extreme obesity and diabetes (28,29). Obesity in mice with the lethal yellow agouti (A^y) mutation is the result of a 170-kb deletion event 5′ of the agouti locus. The deletion causes a chimeric mRNA between the coding region of agouti and the *Raly* 5′ untranslated region, leading to ubiquitous, unregulated expression of agouti protein. The lethal yellow agouti mutation is dominant and homozygous lethal (30–32). Ectopic agouti expression in the hypothalamus leads to chronic antagonism of the melanocortin receptor 4, resulting in mild hyperphagia and late-onset obesity with marked hyperinsulinemia and insulin resistance (32,33). We report herein that expression of Wnt10b in adipose tissue reduces adiposity in the *ob/ob* obesity model by 65–70% at 8 weeks of age. Likewise, mice expressing Wnt10b on the lethal yellow agouti background show a substantial decline in adipose mass, as well as an improvement in glucose tolerance and insulin sensitivity at 5 and 12 months of age. Improved insulin sensitivity in FABP4-Wnt10b mice may be due to decreased activation of macrophages in adipose tissues and reduced expression of resistin, monocyte chemotactic protein (MCP)-1, tumor necrosis factor (TNF)-α, and inducible nitric oxide synthase (iNOS).

RESEARCH DESIGN AND METHODS

All studies were approved by the university committee on use and care of animals, and daily care of mice was overseen by the unit for laboratory animal medicine. Transgenic mice that express mouse Wnt10b under control of the FABP4 promoter (FABP4-Wnt10b) were described previously (14). FABP4-Wnt10b mice bred to C57BL/6 mice (N2-N3) were crossed with B6.Cg-A^y/J mice (The Jackson Laboratory, Bar Harbor, ME), and F1 progeny were used for analyses. Likewise, FABP4-Wnt10b transgenic mice were crossed with B6.V-*Lep*^{ob}/J heterozygous mice (The Jackson Laboratory), and the resulting progeny were interbred and F2 mice used for analyses. Mice had ad libitum access to water and rodent chow (5001 rodent chow; Test Diets, Brentwood, MO).

Glucose and insulin tolerance tests. To test glucose tolerance, mice were given an intraperitoneal injection of 1.5 mg glucose/g body wt after a 16-h fast. Blood glucose was determined at the indicated times from tail blood using the OneTouch Ultra glucometer (Lifescan, Burnaby, Canada). To determine insulin sensitivity, mice were given an intraperitoneal injection of 1.0 unit insulin/kg body wt after a 16-h fast. Tail blood samples were collected at the indicated times, and glucose concentrations were determined as described above.

Adipocyte histology. White adipose tissue was dissected and fixed in 10% neutral buffered formalin for at least 48 h. After embedding in paraffin, adipose tissue sections were stained with hematoxylin and eosin. Images were taken on an Olympus BX-51 microscope with an Olympus DP70 color digital camera. Adobe Photoshop was used to enhance the contrast of the images before analysis. MetaMorph software (version 6.1; Molecular Devices, Downingtown, PA) was used to calculate cellular area and the number of adipocytes per field with integrated morphometry analysis. Treatment differences were analyzed by ANOVA.

Analysis of mRNA expression. Quantitative real-time PCR was performed as described (14,34). Briefly, RNA was isolated from tissues using RNA Stat 60 (Tel-Test, Friendswood, TX) and further purified using an RNeasy kit (Qiagen, Valencia, CA). RNA was treated with DNase I, and cDNA was synthesized using the TaqMan system (Applied Biosystems, Foster City, CA) and random hexamer primers. SYBR Green I dye (Molecular Probes, Madison, WI) was used to monitor amplification of cDNA on the I-Cycler and IQ real-time PCR detection system (Bio-Rad Laboratories, Hercules, CA). 18S rRNA was the reference gene used to normalize cDNA. All primer sequences were validated as described (35) and are reported in Table 1.

Adipocyte isolation. Fat cells were isolated by a procedure modified from that of Rodbell (36). Gonadal adipose tissue was dissected, weighed, placed in ice-cold Krebs-Ringer HEPES buffer, and minced. Adipose tissue was then digested in 5 ml digestion buffer (1X Krebs-Ringer HEPES containing 1–2 mg/ml Collagenase II, C-6885; Sigma Chemical, St. Louis, MO) at 37°C for 45–60 min with continuous shaking (~150 rpm) (4,36). Undigested tissue was removed by filtering through a 100-μm mesh. Adipocytes were separated from stromal vascular cells by low-speed centrifugation. RNA was prepared and analyzed as described above.

Energy expenditure. Measurement of oxygen consumption (V_{O_2}) with indirect calorimetry was performed on mice at 1 year of age. Animals were maintained on 12-h light and dark cycles beginning at 6:00 A.M. and 6:00 P.M., respectively. Mice were acclimated in measuring chambers for 2 weeks before recording. Measurements of V_{O_2} were recorded every 24 min over 4 days using the Oxymax System (Columbus Instruments, Columbus, OH). After 3 days, chow was removed and measurements continued for another day.

Food intake. Mice were housed individually in microisolator cages with wire mesh flooring and acclimated for at least 7 days. Food consumption from 5 consecutive days was used to calculate average daily food intake.

Dual-energy X-ray absorptiometry. Mice were anesthetized using inhaled isoflurane and scanned using the pDEXA Sabre X-ray bone densitometer (Norland Medical Systems, Fort Atkinson, WI). System software estimated fat, lean, and bone mineral mass for each mouse.

Serum hormones. Blood was collected from the tail or orbital plexus and allowed to clot at room temperature for 30 min. Serum was then prepared and stored at −80°C until assayed. Insulin, leptin, resistin, and adiponectin were simultaneously measured on a Luminex 100 machine using the Lincoplex mouse serum adipokine kit according to the manufacturer's protocol (Linco Research, St. Charles, MO). Insulin was assayed in mice at 1 year of age using the Ultra Sensitive Rat Insulin ELISA kit (Crystal Chem, Downers Grove, IL).

Serum lipids. Concentrations of serum nonesterified fatty acids were determined using the Free fatty acid, Half-micro test according to manufacturer's protocol (Roche Diagnostics, Mannheim, Germany). Serum triacylglycerol was determined according to the manufacturer's instructions with the Infinity Triglyceride Reagent kit (Sigma Chemical), using glycerol as the standard. Serum cholesterol was determined using the Infinity Cholesterol Reagent kit (Sigma Chemical).

RESULTS

Wnt10b inhibits development of obesity in *ob/ob* mice. We reported previously that FABP4-Wnt10b transgenic mice resist diet-induced obesity (14). To determine if Wnt10b also inhibits obesity due to leptin deficiency, the FABP4-Wnt10b transgene was transferred onto the *ob/ob* background. While *ob/ob* mice demonstrate early-onset obesity with a 50% increase in body weight compared with wild-type mice at 8 weeks of age, Wnt10b-*ob/ob* mice show a modest, yet statistically insignificant, 11% increase in body weight compared with Wnt10b alone (Fig. 1*A*). As described previously (14), FABP4-Wnt10b mice weigh more than wild-type mice due to increased thickness of skin (Fig. 1*A*). Inspection reveals that Wnt10b-*ob/ob* mice have a remarkable decrease in the epididymal and perirenal adipose depots compared with *ob/ob* mice (Fig. 1*B*). Quantification of tissue weight reveals a 65–70% reduction in visceral and subcutaneous adipose tissue. Although weights of heart, lung, kidneys, and spleen were not different (data not shown), increased weight of pancreas and liver was observed in Wnt10b-*ob/ob* mice (Fig. 1*C*). Profound hepatic steatosis was observed in both *ob/ob* and Wnt10b-*ob/ob* mice (data not shown). Taken together, these data indicate that obesity due to leptin deficiency is inhibited by expression of Wnt10b in adipose tissue.

Wnt10b inhibits obesity in agouti mice. To further investigate the ability of Wnt10b to avert genetic obesity, we crossed FABP4-Wnt10b and lethal yellow agouti (A^y) mice. Ectopic expression of agouti in A^y mice causes mild hyperphagia, late-onset obesity and severe hyperinsulinemia (32,33). In our studies, A^y and Wnt10b-A^y mice had similar body weights at 4 months of age. However, analysis of body composition by dual-energy X-ray absorptiometry

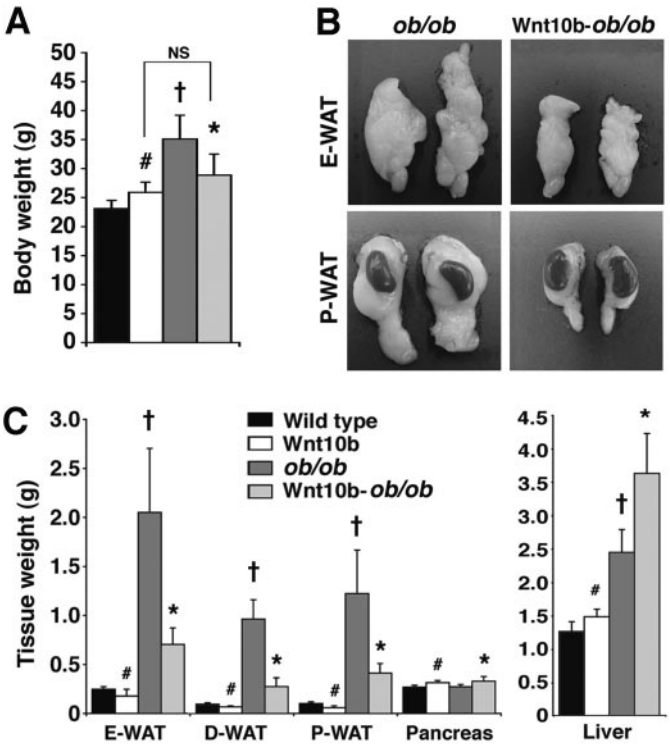

FIG. 1. Wnt10b inhibits development of obesity in *ob/ob* mice. *A*: Body weights of wild-type (n = 9), Wnt10b (n = 8), *ob/ob* (n = 10), and Wnt10b-*ob/ob* (n = 6) mice at ~8 weeks of age. *B*: Isolated epididymal and perirenal fat depots from *ob/ob* and Wnt10b-*ob/ob* mice. *C*: Weights of adipose depots, pancreas, and liver. Body and tissue weights are reported as means ± SD. Statistical analysis was evaluated using Student's t test. #P < 0.05 Wnt10b vs. wild type; †P < 0.05 *ob/ob* vs. wild type; *P < 0.05 Wnt10b-*ob/ob* vs. *ob/ob*. D-WAT, dorsolumbar white adipose tissue; E-WAT, epididymal white adipose tissue; NS, not significant; P-WAT, perirenal white adipose tissue.

(DEXA) revealed a >50% decrease in fat mass in the Wnt10b-A^y mice, with a concomitant increase in lean mass (Fig. 2*A*). Quantification of adipose depots revealed that reduction in total body lipid in Wnt10b-A^y mice was accounted for by decreased white adipose tissue. Weights of visceral and subcutaneous adipose depots in Wnt10b-A^y mice were reduced by 55 and 70%, respectively (Fig. 2*B* and *C*). Average adipocyte size was not different between genotypes (data not shown), consistent with a large body of data indicating that Wnt signaling impairs adipogenesis. Reduced adipose tissue in Wnt10b-A^y was not due to decreased energy intake, as food consumption was similar between genotypes (data not shown). As in *ob/ob* mice (Fig. 1*C*), expression of Wnt10b in A^y mice increases weight of pancreas and liver (Fig. 2*C*). Histological analysis suggests that both genotypes have hepatic steatosis (not shown). Thus, Wnt10b inhibits accumulation of adipose tissue in two distinct genetic models of obesity.

Wnt10b-A^y mice have improved glucose tolerance and insulin sensitivity. In addition to obesity, other hallmarks of the lethal yellow agouti phenotype are glucose intolerance, hyperinsulinemia, and insulin resistance (32,37,38). Given the well-known relationship between adiposity and insulin resistance, as well as the reduced amounts of adipose tissue and increased liver and pancreas weights in Wnt10b-A^y mice, we performed experiments to investigate glucose homeostasis in these mice. Random-fed Wnt10b-A^y and A^y littermates were both hyperinsulinemic and exhibited similar blood glucose con-

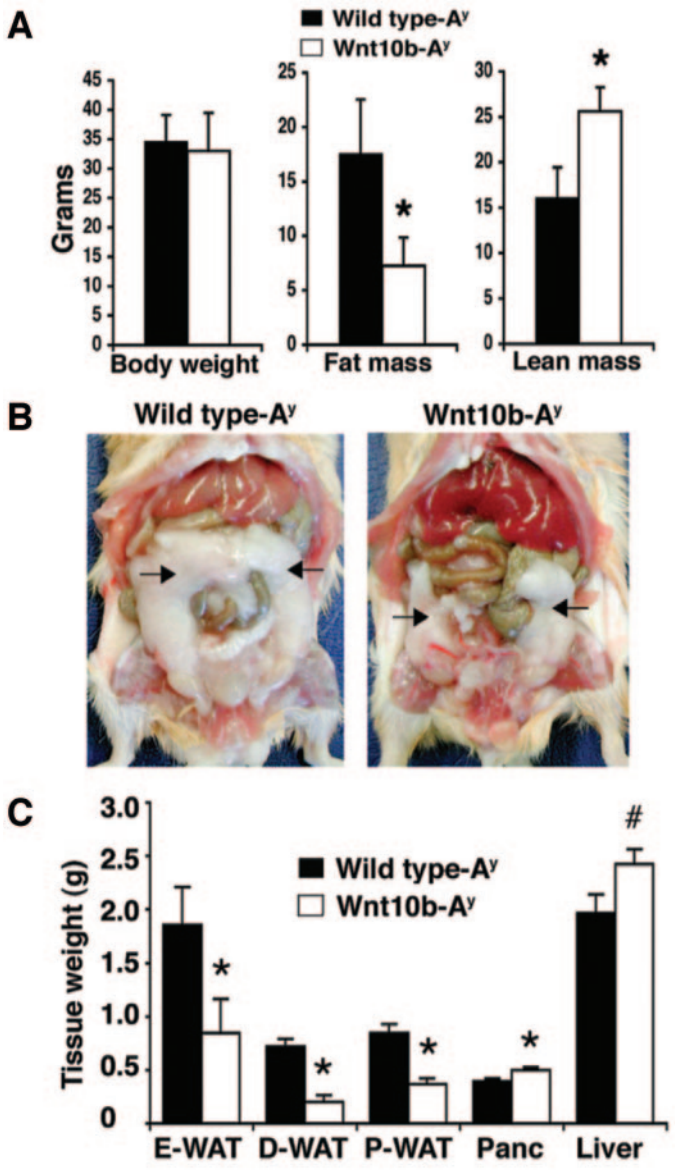

FIG. 2. Wnt10b inhibits obesity in agouti mice. *A*: Body composition of wild-type–A^y and Wnt10b-A^y male mice ($n = 8$) by DEXA at 5 months of age. *B*: Ventral view of representative wild-type–A^y and Wnt10b-A^y mice. Expression of Wnt10b reduces epididymal adipose tissue (arrows). *C*: Weights of adipose depots, pancreas, and liver. Data are presented as means ± SD. Statistical significance was evaluated using Student's *t* test. #$P < 0.05$; *$P < 0.01$. D-WAT, dorsolumbar white adipose tissue; E-WAT, epididymal white adipose tissue; Panc, pancreas; P-WAT, perirenal white adipose tissue.

centrations (Fig. 3*A*). To assess glucose tolerance, mice were subjected to an intraperitoneal glucose challenge (Fig. 3*B*). While A^y mice are glucose intolerant, Wnt10b-A^y mice had significantly lower blood glucose levels at fasted baseline and at every time point thereafter. Although both A^y and Wnt10b-A^y mice were relatively insensitive to insulin, blood glucose levels in Wnt10b-A^y mice were lower than in A^y mice at each time point after administration of insulin (Fig. 3*C*). While blood glucose from A^y mice failed to fall below baseline during the assay, littermate Wnt10b-A^y mice showed a decline in blood glucose observed 45 min after intraperitoneal insulin challenge (Fig. 3*C*). Therefore, expression of Wnt10b in adipose tissue improves whole-body glucose homeostasis in genetically obese mice, similar to results observed with diet-induced obesity (14).

To gain insight into potential causes of improved glucose tolerance and insulin sensitivity, we evaluated the levels of key serum adipokines. Consistent with previous results in nonagouti mice (14), Wnt10b-A^y mice had a 22% reduction in total adiponectin compared with A^y mice (Fig. 3*D*). In addition, Wnt10b-A^y mice showed a 63% reduction in leptin, correlating with reduced adipose tissue mass. Notably, resistin levels in serum and expression of resistin in adipose tissue were decreased in Wnt10b-A^y mice (Fig. 3*D* and *E*), possibly contributing to improved glucose tolerance.

It has been proposed that obesity-related insulin resistance is secondary to chronic inflammation in adipose tissue (39–43). Thus, we next examined expression of proinflammatory genes in epididymal adipose tissue of A^y and Wnt10b-A^y mice. Interleukin-6 and TNF-α are two proinflammatory cytokines commonly elevated in obesity and both have been implicated in insulin resistance (39). While interleukin-6 was similarly expressed in Wnt10b-A^y mice (data not shown), expression of TNF-α mRNA was reduced by ~50% compared with A^y mice (Fig. 3*E*). Obesity is accompanied by increased expression of the chemokine MCP-1 in adipose tissue, where MCP-1 plays a roll in recruiting macrophages and stimulating insulin resistance (44). Our assessment of mRNA levels of MCP-1 revealed that expression of MCP-1 is decreased in Wnt10b-A^y mice. While only a trend toward reduced expression of F4/80 was also noted (not shown), iNOS expression, one possible mediator of inflammation-associated insulin resistance (43,45), is reduced by 73% in white adipose tissue of Wnt10b-A^y mice (Fig. 3*E*). Thus, improved glucose tolerance and insulin sensitivity in Wnt10b-*A* mice may be due, in part, to reduced recruitment and/or activation of resident macrophage and decreased inflammation in adipose tissue.

Reduced inflammation of adipose tissue from Wnt10b-A^y mice at 1 year of age. Expansion of adipose tissue mass in agouti mice occurs relatively gradually, with severe obesity observed only later in life. To assess whether Wnt10b continues to provide protection against obesity with age, we compared phenotypes of female A^y and Wnt10b-A^y mice at 1 year of age. Whereas agouti mice gained >20 g of weight between 5 and 12 months of age, weights of Wnt10b-A^y mice remained relatively constant, with Wnt10b-A^y weighing ~40% less than A^y littermates by 12 months of age (Fig. 4*A*). The reduction in body weight is largely due to a striking decrease in visceral and subcutaneous adipose depots, with 80–90% less ovarian, perirenal, and dorso-lumbar adipose tissue (Fig. 4*A*). These data indicate that Wnt10b-A^y mice resist late-onset obesity associated with the agouti mutation.

Histomorphometric analysis was used to establish that the decrease in adipose tissue weight (Fig. 4*A*) was not due to decreased adipocyte size (Fig. 4*B*). Furthermore, molecular characterization of adipocytes isolated from Wnt10b-A^y mice revealed that many adipocyte genes are expressed normally, with the notable exception of resistin, which was decreased by 85% (Fig. 4*C*). Taken together, these data suggest that protection against genetic obesity by Wnt10b is through a reduction in adipocyte number rather than altered adipocyte metabolism and or function.

Analysis of blood glucose and serum insulin at 12 months showed no difference in the fed state; however, a slight decrease in blood glucose and a substantial 60%

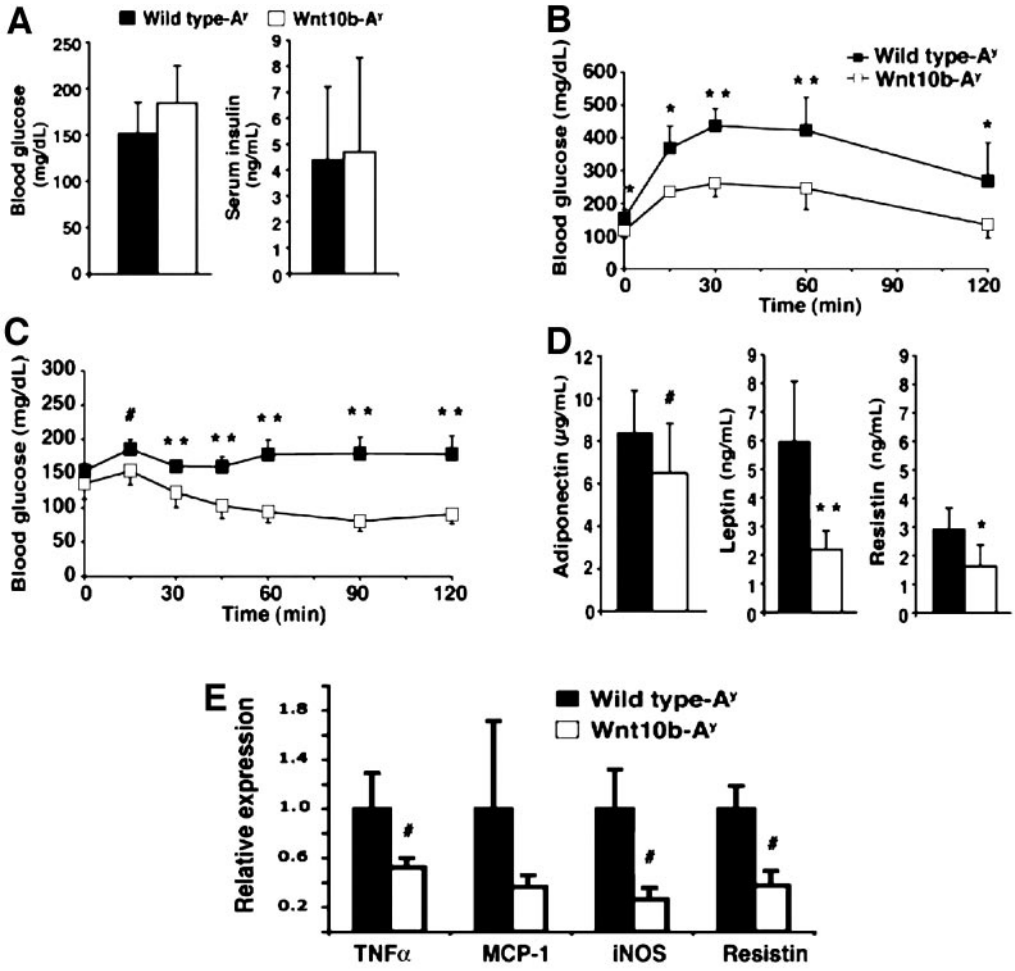

FIG. 3. Wnt10b-A^y mice have improved glucose tolerance and insulin sensitivity. *A*: Concentrations of blood glucose and serum insulin in random-fed male mice at 5 months of age ($n = 6$). Male A^y ($n = 6$) and Wnt10b-A^y ($n = 7$) mice at 5 months of age were fasted overnight before intraperitoneal administration of glucose or insulin. *B*: Glucose tolerance test. *C*: Insulin tolerance test. Data from glucose and insulin tolerance assays were analyzed by two-way ANOVA and baseline values analyzed using Student's *t* test. *D*: Serum adipokines from random-fed A^y and Wnt10b-A^y mice ($n = 6$). All values in *A–D* are reported as means ± SD. *E*: Expression of indicated genes in epididymal white adipose tissue ($n = 4$) was evaluated by quantitative RT-PCR. Wnt10b-A^y is shown relative to wild type–A^y (means ± SE). #$P < 0.05$; *$P < 0.01$; **$P < 0.001$.

decrease in serum insulin in the fasted state suggest that Wnt10b-A^y mice remain more sensitive to insulin as they age (Fig. 4*D*). Analysis of adipokines revealed a 30–50% reduction in serum leptin, an ~98% decrease in serum resistin, and a 55–70% reduction in total adiponectin in Wnt10b-A^y mice. Analyses of serum lipids showed no statistical change in triglyceride or free fatty acid concentrations (Table 2). As observed at 6 months of age, Wnt10b-A^y mice show a dramatic decrease in expression of MCP-1, F4/80, and iNOS mRNAs in perirenal adipose tissue at 12 months of age, although altered TNF-α was not observed (Fig. 4*E*). Thus, decreased inflammation in adipose tissue of Wnt10b-A^y mice is a possible basis for improved insulin sensitivity in these mice as they age.

Energy balance at 1 year of age. We next investigated energy balance in A^y and Wnt10b-A^y mice to determine if altered food intake or oxygen consumption contributed to the ability of Wnt10b-A^y mice to resist expansion of their adipose tissues with age. As expected based on analysis of younger A^y and Wnt10b-A^y mice, as well as prior analysis of FABP4-Wnt10b mice (14), food consumption was not altered by the Wnt10b transgene (Fig. 5*A*; not shown), although a trend toward reduced intake was observed. We then used indirect calorimetry to investigate oxygen consumption and respiratory quotient. There was no significant change in total oxygen consumption under random-fed or fasted conditions (Fig. 5*B*). Furthermore, respiratory quotient (Fig. 5*B*) under random-fed and fasted conditions was similar between genotypes. By DEXA, Wnt10b-A^y mice have far less adipose mass but have a surprising increase in lean mass that is not accounted for by weights of individual muscles or other tissues/organs (Fig. 5*C* and Table 2). Taken together, it appears likely that differences in body weight and accumulation of adipose tissue are due to very small, insensible changes in energy balance as these mice age.

DISCUSSION

In addition to decreasing adiposity, activation of Wnt signaling in Wnt10b-A^y greatly improves glucose homeostasis due to improved insulin sensitivity (Fig. 3). Similar findings were observed with FABP4-Wnt10b mice on a chow or high-fat diet (14). Based on analysis of glucose homeostasis in mice with tissue-selective loss of insulin receptors, it is likely that improved insulin sensitivity decreases hepatic glucose production in Wnt10b-A^y mice; however, euglycemic-hyperinsulinemic clamp stud-

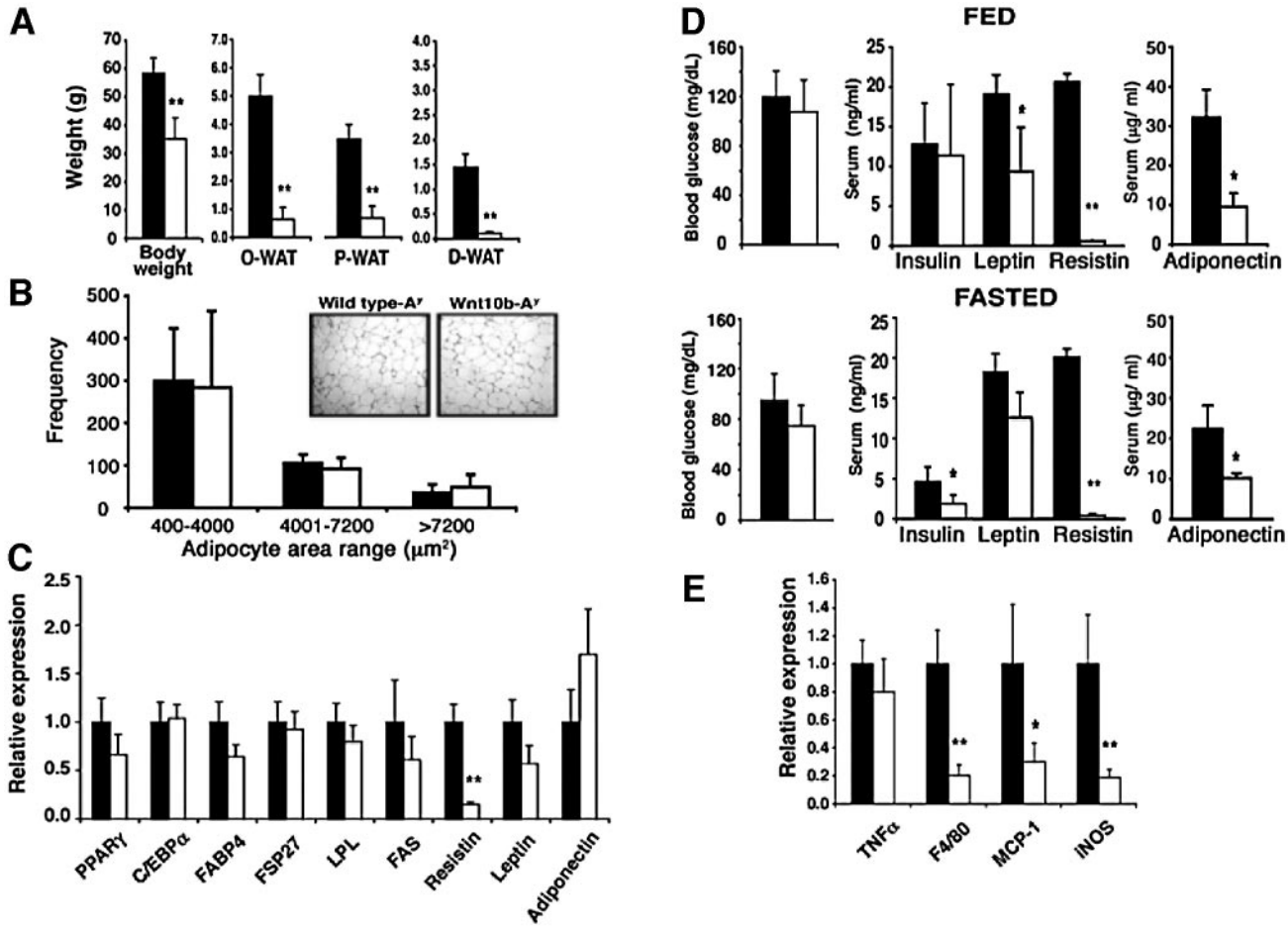

FIG. 4. Resistance to obesity in Wnt10b-A^y mice at 1 year of age. Female wild-type–A^y and Wnt10b-A^y mice at 12 months of age were random fed or fasted overnight ($n = 4$). *A*: Body and adipose depot weights. D-WAT, dorsolumbar white adipose tissue; O-WAT, ovarian white adipose tissue; P-WAT, perirenal white adipose tissue. *B*: Adipocyte area analysis and representative pictures of microscopic fields. *C*: Primary adipocytes were isolated from ovarian adipose tissue from wild-type–A^y and Wnt10b-A^y mice ($n = 8$). Gene expression was evaluated by quantitative RT-PCR for the indicated genes. Wnt10b-A^y is shown relative to wild type–A^y (means ± SE). C/EBP, CCAAT/enhancer-binding protein; FABP, fatty acid–binding protein 4; FAS, fatty acid synthase; FSP, fat-specific protein; LPL, lipoprotein lipase; PPAR, peroxisome proliferator–activated receptor. *D*: Blood glucose and serum proteins from random-fed ($n = 4$) and fasted ($n = 4$) mice. *E*: Quantitative RT-PCR of mRNA from perirenal adipose tissue comparing wild-type–A^y ($n = 8$) and Wnt10b-A^y ($n = 8$) mice. Statistical significance was evaluated using Student's *t* test. *$P < 0.05$; **$P < 0.001$.

ies will be required to confirm this hypothesis. Surprisingly, phosphorylation of Akt in liver and muscle 5 min after administration of insulin to wild-type or FABP4-Wnt10b mice is not altered (data not shown), suggesting a mechanism downstream of Akt. While at 1 year of age, absolute weights of liver and pancreas are not different between genotypes, Wnt10b-A^y mice have larger livers and pancreata when expressed relative to total body weight. This idea is supported by increased size of these organs when the Wnt10b transgene is expressed on a mixed genetic background (14) or in the absence of leptin (Fig. 1). As observed in mice deficient for lipin (46), hepatocytes in FABP4-Wnt10b mice transiently accumulate neutral lipid in the postnatal period (not shown); however, our analysis of liver glycogen, lipid content, total protein, and tissue morphology later in life did not reveal altered composition (not shown). Thus, it may be that some of the improved glucose homeostasis comes from increased metabolic capacity of liver and pancreas. Whether Wnt signaling influences the chalone that regulates size of liver or pancreas will require additional study.

Our analysis of energy balance in A^y and Wnt10b-A^y mice led to paradoxical findings. While a trend toward reduced food intake was observed, there was no significant change in total oxygen consumption under random-fed or fasted conditions (Fig. 5*B*). In addition, Wnt10b-A^y mice consumed similar amounts of oxygen throughout the day (not shown), providing further evidence that Wnt10b-A^y mice do not differentially enter torpor while in the postabsorptive state, nor that the lack of brown adipose tissue in FABP4-Wnt10b mice influences oxygen consumption under these conditions (14). Average respiratory quotient (Fig. 5*B*) under random-fed and fasted conditions was similar between genotypes, suggesting that oxidation of fuels is regulated normally in Wnt10b-A^y mice. However, the normal fluctuations over a 24-h period were blunted in Wnt10b-A^y mice (not shown), perhaps due to increased nibbling throughout the day or decreased metabolic flexibility. Although expressing oxygen consumption relative to body mass$^{0.75}$ suggests that Wnt10b-A^y mice have reduced body weight due to increased metabolic rate, this may not be appropriate in light of the large differences in body composition (Fig. 5*C*). However, given the large increase in apparent lean mass, normalizing oxygen consumption to lean body mass gives the paradoxical finding that Wnt10b-A^y mice have reduced metabolic

TABLE 2
Tissue weights and serum lipids of fed or fasted female mice at 12 months of age (n = 4)

	Wild type–A^y	Wnt10b-A^y	Change	P value
Fed				
Body weight (g)	60.1 ± 4.4	36.9 ± 10.1	−39%	0.0055
Length (cm)	10.73 ± 0.29	10.33 ± 0.57		0.25
E-WAT (g)	4.94 ± 0.98	0.71 ± 0.60	−86%	0.0003
D-WAT (g)	1.64 ± 0.18	0.08 ± 0.01	−95%	0.006
P-WAT (g)	3.45 ± 0.33	0.81 ± 0.55	−77%	0.0002
BAT (g)	2.40 ± 0.47	0.73 ± 0.64	−70%	0.006
Pancreas (g)	0.41 ± 0.06	0.48 ± 0.04		0.15
Liver (g)	2.52 ± 0.15	2.58 ± 0.80		0.89
Spleen (g)	0.13 ± 0.04	0.28 ± 0.07	+2-fold	0.008
Kidneys (g)	0.49 ± 0.03	0.49 ± 0.09		0.92
Heart (g)	0.18 ± 0.008	0.19 ± 0.009		0.34
Serum TGs (mg/dl)	129.33 ± 20.20	117.57 ± 54.83		0.70
Serum FFAs (mmol/l)	0.10 ± 0.024	0.11 ± 0.017		0.42
Serum cholesterol (mg/dl)	125.12 ± 14.45	90.39 ± 15.54	−28%	0.017
Fasted				
Body weight (g)	56.4 ± 6.5	33.7 ± 3.9	−40%	0.0009
Length (cm)	10.9 ± 0.32	10.5 ± 0.37		0.15
E-WAT (g)	5.05 ± 0.63	0.56 ± 0.18	−89%	0.0001
D-WAT (g)	1.34 ± 0.27	0.12 ± 0.04	−91%	0.0001
P-WAT (g)	3.49 ± 0.73	0.56 ± 0.25	−84%	0.0002
BAT (g)	2.33 ± 0.68	0.48 ± 0.15	−83%	0.006
Pancreas (g)	0.38 ± 0.06	0.41 ± 0.05		0.41
Liver (g)	2.10 ± 0.20	2.09 ± 0.29		0.96
Spleen (g)	0.14 ± 0.05	0.22 ± 0.06	+57%	0.09
Kidneys (g)	0.47 ± 0.01	0.43 ± 0.04		0.17
Heart (g)	0.19 ± 0.03	0.19 ± 0.02		0.86
Serum TGs (mg/dl)	81.64 ± 21.04	67.44 ± 9.02		0.26
Serum FFAs (mmol/l)	0.22 ± 0.19	0.13 ± 0.07		0.39
Serum cholesterol (mg/dl)	161.64 ± 40.29	129.85 ± 14.86		0.19

Data are means ± SD. BAT, brown adipose tissue; D-WAT, dorsolumbar white adipose tissue; E-WAT, epididymal white adipose tissue; FFA, free fatty acid; P-WAT, perirenal white adipose tissue; TG, triglyceride.

rate (Fig. 5*C*). While the profound alterations in fat content of the Wnt10b-A^y mice as assessed by DEXA are closely aligned with our measurements of adipose tissue weights, the source of increased lean mass in Wnt10b-A^y mice remains elusive as the additional 10 g of "nonfat nonmineral" mass cannot be explained by the weights of individual muscles or other tissues/organs (Fig. 5*C* and Table 2), perhaps suggesting that Wnt signaling in this context alters hemodynamics to increase total water content. Some of the lean mass may also be from weight of skin, which although not measured in this experiment, is increased in FABP4-Wnt10b mice (14).

Our analyses of adipokine expression suggests that while expression of adiponectin and leptin are not changed on a per-adipocyte basis (Fig. 4*C*), circulating levels of both of these factors are decreased in serum (Figs. 3 and 4). Based on these experiments, improved glucose tolerance is unlikely to be associated with either adiponectin or leptin, although differential sensitivity to these factors cannot be ruled out. A caveat of this experiment is that we measured total adiponectin; thus, we do not have a measure of the more biologically active higher-order forms (47). Additionally, increased insulin sensitivity could be due, in part, to the striking decrease in expression of resistin in adipocytes and adipose tissue and the corresponding lower levels in circulation (48) (Figs. 3 and 4). Although resistin may contribute to increased insulin sensitivity in Wnt10b-A^y mice, improved glucose homeostasis is more likely associated with decreased inflammation in adipose tissue, as assessed by expression of F4/80 and iNOS (Figs. 3 and 4). Fewer macrophages could be secondary to inhibition of obesity (39,40,49), and the corresponding decrease in expression of MCP-1 (Figs. 3 and 4) from preadipocytes, endothelial cells, and adipocytes (42). Reduced MCP-1 in Wnt10b-A^y mice may also influence insulin sensitivity independent of macrophage recruitment, as exposure of differentiated 3T3-L1 adipocytes to MCP-1 decreases expression of adipocyte genes, including GLUT4 and peroxisome proliferator–activated receptor γ, and impairs insulin-stimulated glucose uptake (42). Although controversial (50), decreased signaling by the MCP-1 receptor, CCR2 (C-C motif chemokine receptor-2), has been reported to improve insulin sensitivity and glucose homeostasis in obese mice (51). Alternatively, macrophage development or activation could be influenced by expression of Wnt10b in bone marrow, macrophages, or adipose tissue. Along with decreased MCP-1, we observed that TNF-α, an inflammatory cytokine well known for stimulating insulin resistance in adipose tissue, is expressed at lower levels in 6-month-old mice. Consistent with decreased activity of inflammatory cytokines, we observed decreased expression of a downstream target, iNOS, at both 6 months and 1 year of age (Figs. 3 and 4). iNOS is normally elevated in adipose tissues and muscle of

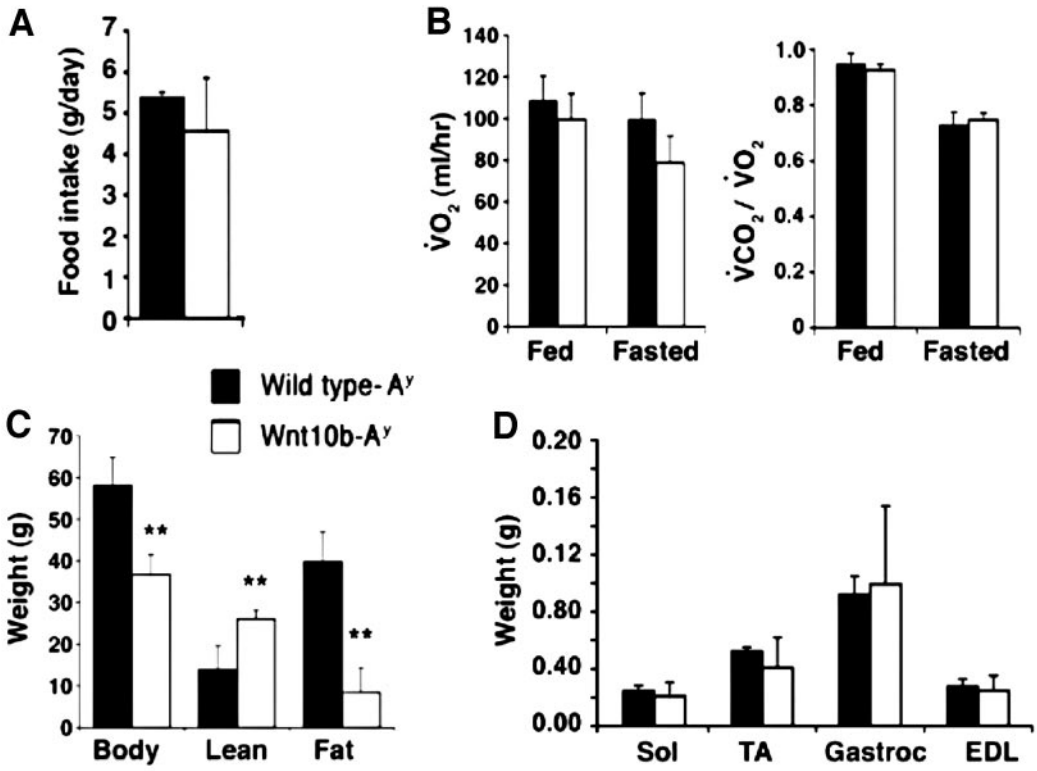

FIG. 5. Analysis of energy balance at 1 year of age. *A*: Food consumption of individually caged female mice. *B*: Oxygen consumption (Vo_2) and carbon dioxide production ($V\text{co}_2$) using indirect calorimetry from female A^y and Wnt10b-A^y mice. *C*: Body composition of mice determined by DEXA. *D*: Weights of individual leg muscles. EDL, extensor digitorum longus; Gastroc, gastrocnemius; Sol, soleus; TA, tibialis anterior. All data are expressed as means ± SD (n = 4–8). Statistical significance was evaluated using Student's t test. **$P < 0.001$.

genetic and dietary models of obesity (43) and is associated with insulin resistance in muscle. Thus, improved glucose homeostasis in Wnt10b-A^y mice is probably caused by reduced resistin and decreased recruitment and activation of macrophages in adipose tissues. Alternatively, increased Wnt10b signaling in adipose tissue may alter whole-body insulin sensitivity through a unique mechanism.

ACKNOWLEDGMENTS

This work was supported by grants from the National Institutes of Health to O.A.M. (DK51563 and DK62876). Other support was from the Nathan Shock Mutant and Transgenic Rodent Core. Fellowships were from Tissue Engineering and Regeneration Training Grant, Center for Organogenesis, a Rackham predoctoral fellowship, a mentor-based postdoctoral fellowship from the American Diabetes Association, and the Belgian Fonds National de la Recherche Scientifique. This work used the Morphology and Image Analysis Core of the Michigan Diabetes Research and Training Center, which is funded by NIH5P60 DK20572 from the National Institute of Diabetes and Digestive and Kidney Diseases of the National Institutes of Health.

REFERENCES

1. MacDougald OA, Mandrup S: Adipogenesis: forces that tip the scales. *Trends Endocrinol Metab* 13:5–11, 2002
2. Ross SE, Hemati N, Longo KA, Bennett CN, Lucas PC, Erickson RL, MacDougald OA: Inhibition of adipogenesis by Wnt signaling. *Science* 289:950–953, 2000
3. Ross SE, Erickson RL, Gerin I, DeRose PM, Bajnok L, Longo DA, Misek DE, Kuick R, Hanask SM, Atkins KB, Maehle S, Nebb HI, Madsen L, Kristiansen K, MacDougald OA: Microarray analyses during adipogenesis: understanding the effects of Wnt-signaling on adipogenesis and the roles of LXRa in adipocyte metabolism. *Mol Cell Biol* 22:5989–5999, 2002
4. Bennett CN, Ross SE, Longo KA, Bajnok L, Hemati N, Johnson KW, Harrison SD, MacDougald OA: Regulation of Wnt signaling during adipogenesis. *J Biol Chem* 277:30998–31004, 2002
5. Longo KA, Kennell JA, Ochocinska MJ, Ross SE, Wright WS, MacDougald OA: Wnt signaling protects 3T3–L1 preadipocytes from apoptosis through induction of insulin-like growth factors. *J Biol Chem* 277:38239–38244, 2002
6. Gustafson B, Smith U: Cytokines promote Wnt signaling and inflammation and impair the normal differentiation and lipid accumulation in 3T3–L1 preadipocytes. *J Biol Chem* 281:9507–9516, 2006
7. Kennell JA, MacDougald OA: Wnt signaling inhibits adipogenesis through beta-catenin-dependent and -independent mechanisms. *J Biol Chem* 280: 24004–24010, 2005
8. Logan CY, Nusse R: The Wnt signaling pathway in development and disease. *Annu Rev Cell Dev Biol* 20:781–810, 2004
9. Moon RT, Kohn AD, De Ferrari GV, Kaykas A: WNT and beta-catenin signalling: diseases and therapies. *Nat Rev Genet* 5:691–701, 2004
10. Westendorf JJ, Kahler RA, Schroeder TM: Wnt signaling in osteoblasts and bone diseases. *Gene* 341:19–39, 2004
11. Bennett CN, Longo KA, Wright WS, Suva LJ, Lane TF, Hankenson KD, Macdougald OA: Regulation of osteoblastogenesis and bone mass by Wnt10b. *Proc Natl Acad Sci U S A* 102:3324–3329, 2005
12. Jackson A, Vayssiere B, Garcia T, Newell W, Baron R, Roman-Roman S, Rawadi G: Gene array analysis of Wnt-regulated genes in C3H10T1/2 cells. *Bone* 36:585–598, 2005
13. Moldes M, Zuo Y, Morrison RF, Silva D, Park BH, Liu J, Farmer SR: Peroxisome-proliferator-activated receptor gamma suppresses Wnt/beta-catenin signalling during adipogenesis. *Biochem J* 376:607–613, 2003
14. Longo KA, Wright WS, Kang S, Gerin I, Chiang SH, Lucas PC, Opp MR, MacDougald OA: Wnt10b inhibits development of white and brown adipose tissues. *J Biol Chem* 279:35503–35509, 2004
15. Clement-Lacroix P, Ai M, Morvan F, Roman-Roman S, Vayssiere B, Belleville C, Estrera K, Warman ML, Baron R, Rawadi G: Lrp5-independent activation of Wnt signaling by lithium chloride increases bone formation and bone mass in mice. *Proc Natl Acad Sci U S A* 102:17406–17411, 2005
16. Bodine PV, Zhao W, Kharode YP, Bex FJ, Lambert AJ, Goad MB, Gaur T, Stein GS, Lian JB, Komm BS: The Wnt antagonist secreted frizzled-related

protein-1 is a negative regulator of trabecular bone formation in adult mice. *Mol Endocrinol* 18:1222–1237, 2004
17. Koza RA, Nikonova L, Hogan J, Rim JS, Mendoza T, Faulk C, Skaf J, Kozak LP: Changes in gene expression foreshadow diet-induced obesity in genetically identical mice. *PLoS Genet* 2:e81, 2006
18. Christodoulides C, Laudes M, Cawthorn WP, Schinner S, Soos M, O'Rahilly S, Sethi JK, Vidal-Puig A: The Wnt antagonist Dickkopf-1 and its receptors are coordinately regulated during early human adipogenesis. *J Cell Sci* 119:2613–2620, 2006
19. Taylor-Jones JM, McGehee RE, Rando TA, Lecka-Czernik B, Lipschitz DA, Peterson CA: Activation of an adipogenic program in adult myoblasts with age. *Mech Ageing Dev* 123:649–661, 2002
20. Vertino AM, Taylor-Jones JM, Longo KA, Bearden ED, Lane TF, McGehee RE Jr, MacDougald OA, Peterson CA: Wnt10b deficiency promotes coexpression of myogenic and adipogenic programs in myoblasts. *Mol Biol Cell* 16:2039–2048, 2005
21. Akimoto T, Ushida T, Miyaki S, Akaogi H, Tsuchiya K, Yan Z, Williams RS, Tateishi T: Mechanical stretch inhibits myoblast-to-adipocyte differentiation through Wnt signaling. *Biochem Biophys Res Commun* 329:381–385, 2005
22. Christodoulides C, Scarda A, Granzotto M, Milan G, Dalla Nora E, Keogh J, De Pergola G, Stirling H, Pannacciulli N, Sethi JK, Federspil G, Vidal-Puig A, Farooqi IS, O'Rahilly S, Vettor R: WNT10B mutations in human obesity. *Diabetologia* 49:678–684, 2006
23. Tseng YH, Kriauciunas KM, Kokkotou E, Kahn CR: Differential roles of insulin receptor substrates in brown adipocyte differentiation. *Mol Cell Biol* 24:1918–1929, 2004
24. Tseng YH, Butte AJ, Kokkotou E, Yechoor VK, Taniguchi CM, Kriauciunas KM, Cypess AM, Niinobe M, Yoshikawa K, Patti ME, Kahn CR: Gene-expression in brown preadipocytes predicts differentiation: role of insulin receptor substrates and necdin. *Nat Cell Biol* 7:601–611, 2005
25. Kanazawa A, Tsukada S, Sekine A, Tsunoda T, Takahashi A, Kashiwagi A, Tanaka Y, Babazono T, Matsuda M, Kaku K, Iwamoto Y, Kawamori R, Kikkawa R, Nakamura Y, Maeda S: Association of the gene encoding wingless-type mammary tumor virus integration-site family member 5B (WNT5B) with type 2 diabetes. *Am J Hum Genet* 75:832–843, 2004
26. Kanazawa A, Tsukada S, Kamiyama M, Yanagimoto T, Nakajima M, Maeda S: Wnt5b partially inhibits canonical Wnt/beta-catenin signaling pathway and promotes adipogenesis in 3T3–L1 preadipocytes. *Biochem Biophys Res Commun* 330:505–510, 2005
27. Arango NA, Szotek PP, Manganaro TF, Oliva E, Donahoe PK, Teixeira J: Conditional deletion of beta-catenin in the mesenchyme of the developing mouse uterus results in a switch to adipogenesis in the myometrium. *Dev Biol* 288:276–283, 2005
28. Ingalls AM, Dickie MM, Snell GD: Obese, a new mutation in the house mouse. *J Hered* 41:317–318, 1950
29. Haluzik M, Colombo C, Gavrilova O, Chua S, Wolf N, Chen M, Stannard B, Dietz KR, Le Roith D, Reitman ML: Genetic background (C57BL/6J versus FVB/N) strongly influences the severity of diabetes and insulin resistance in ob/ob mice. *Endocrinology* 145:3258–3264, 2004
30. Duhl DM, Stevens ME, Vrieling H, Saxon PJ, Miller MW, Epstein CJ, Barsh GS: Pleiotropic effects of the mouse lethal yellow (Ay) mutation explained by deletion of a maternally expressed gene and the simultaneous production of agouti fusion RNAs. *Development* 120:1695–1708, 1994
31. Miller MW, Duhl DM, Vrieling H, Cordes SP, Ollmann MM, Winkes BM, Barsh GS: Cloning of the mouse agouti gene predicts a secreted protein ubiquitously expressed in mice carrying the lethal yellow mutation. *Genes Dev* 7:454–467, 1993
32. Wolff GL, Roberts DW, Mountjoy KG: Physiological consequences of ectopic agouti gene expression: the yellow obese mouse syndrome. *Physiol Genomics* 1:151–163, 1999
33. Yen TT, Gill AM, Frigeri LG, Barsh GS, Wolff GL: Obesity, diabetes, and neoplasia in yellow A(vy)/- mice: ectopic expression of the agouti gene. *FASEB J* 8:479–488, 1994
34. Gerin I, Dolinsky VW, Shackman JG, Kennedy RT, Chiang SH, Burant CF, Steffensen KR, Gustafsson JA, MacDougald OA: LXRbeta is required for adipocyte growth, glucose homeostasis, and beta cell function. *J Biol Chem* 280:23024–23031, 2005
35. Pfaffl MW: A new mathematical model for relative quantification in real-time RT-PCR. *Nucleic Acids Res* 29:e45, 2001
36. Rodbell M: Metabolism of isolated fat cells I. effects of hormones on glucose metabolism and lipolysis. *J Biol Chem* 239:375–380, 1964
37. Masuzaki H, Ogawa Y, Aizawa-Abe M, Hosoda K, Suga J, Ebihara K, Satoh N, Iwai H, Inoue G, Nishimura H, Yoshimasa Y, Nakao K: Glucose metabolism and insulin sensitivity in transgenic mice overexpressing leptin with lethal yellow agouti mutation: usefulness of leptin for the treatment of obesity-associated diabetes. *Diabetes* 48:1615–1622, 1999
38. Mynatt RL, Miltenberger RJ, Klebig ML, Zemel MB, Wilkinson JE, Wilkinson WO, Woychik RP: Combined effects of insulin treatment and adipose tissue-specific agouti expression on the development of obesity. *Proc Natl Acad Sci U S A* 94:919–922, 1997
39. Xu H, Barnes GT, Yang Q, Tan G, Yang D, Chou CJ, Sole J, Nichols A, Ross JS, Tartaglia LA, Chen H: Chronic inflammation in fat plays a crucial role in the development of obesity-related insulin resistance. *J Clin Invest* 112:1821–1830, 2003
40. Weisberg SP, McCann D, Desai M, Rosenbaum M, Leibel RL, Ferrante AW Jr: Obesity is associated with macrophage accumulation in adipose tissue. *J Clin Invest* 112:1796–1808, 2003
41. Uysal KT, Wiesbrock SM, Marino MW, Hotamisligil GS: Protection from obesity-induced insulin resistance in mice lacking TNF-alpha function. *Nature* 389:610–614, 1997
42. Sartipy P, Loskutoff DJ: Monocyte chemoattractant protein 1 in obesity and insulin resistance. *Proc Natl Acad Sci U S A* 100:7265–7270, 2003
43. Perreault M, Marette A: Targeted disruption of inducible nitric oxide synthase protects against obesity-linked insulin resistance in muscle. *Nat Med* 7:1138–1143, 2001
44. Kanda H, Tateya S, Tamori Y, Kotani K, Hiasa K-I, Kitazawa R, Kitazawa S, Miyachi H, Maeda S, Egashira K, Kasuga M: MCP-1 contributes to macrophage infiltration into adipose tissue, insulin resistance, and hepatic steatosis in obesity. *J Clin Invest* 116:1494–1505, 2006
45. Pilon G, Dallaire P, Marette A: Inhibition of inducible nitric-oxide synthase by activators of AMP-activated protein kinase: a new mechanism of action of insulin-sensitizing drugs. *J Biol Chem* 279:20767–20774, 2004
46. Rehnmark S, Giometti CS, Slavin BG, Doolittle MH, Reue K: The fatty liver dystrophy mutant mouse: microvesicular steatosis associated with altered expression levels of peroxisome proliferator-regulated proteins. *J Lipid Res* 39:2209–2217, 1998
47. Trujillo ME, Scherer PE: Adiponectin: journey from an adipocyte secretory protein to biomarker of the metabolic syndrome. *J Int Med* 257:167–175, 2005
48. Steppan CM, Bailey ST, Bhat S, Brown EJ, Banerjee RR, Wright CM, Patel HR, Ahima RS, Lazar MA: The hormone resistin links obesity to diabetes. *Nature* 409:307–312, 2001
49. Cancello R, Henegar C, Viguerie N, Taleb S, Poitou C, Rouault C, Coupaye M, Pelloux V, Hugol D, Bouillot JL, Bouloumie A, Barbatelli G, Cinti S, Svensson PA, Barsh GS, Zucker JD, Basdevant A, Langin D, Clement K: Reduction of macrophage infiltration and chemoattractant gene expression changes in white adipose tissue of morbidly obese subjects after surgery-induced weight loss. *Diabetes* 54:2277–2286, 2005
50. Chen A, Mumick S, Zhang C, Lamb J, Dai H, Weingarth D, Mudgett J, Chen H, MacNeil DJ, Reitman ML, Qian S: Diet induction of monocyte chemoattractant protein-1 and its impact on obesity. *Obes Res* 13:1311–1320, 2005
51. Weisberg SP, Hunter D, Huber R, Lemieux J, Slaymaker S, Vaddi K, Charo I, Leibel RL, Ferrante AW: CCR2 modulates inflammatory and metabolic effects of high-fat feeding. *J Clin Invest* 116:115–124, 2006